# Inverted Induction Motor and Test Stand

Vicente Climente-Alarcón[1], Rubén Puche-Panadero[1], Joan Pons-Llinares[1] and Martín Riera-Guasp[1]

[1] Departamento de Ingeniería Eléctrica
E.T.S.I.I., Universidad Politécnica de Valencia
Departamento de ingeniería Eléctrica. Apdo 22012.
Camino de Vera, s/n; 46022 Valencia
Tel.:+34 96 387 70 00, e-mail: **viclial@csa.upv.es**, **rupucpa@die.upv.es**, **joaponll@etsii.upv.es**, **mriera@die.upv.es**.

**Keywords:** test bed, predictive maintenance, induction motor broken bar detection, model, wavelet transform

## Abstract:

This paper proposes the construction of an inverted induction motor (with the cage winding at the stator), and the test stand associated, to readily monitor rotor parameters and reproduce defects with the intention of optimizing and comparing different techniques of simulation and fault detection.

In order to obtain the level of detail needed for these studies in the working parameters of the operation of a squirrel cage induction motor, full capacity for performing measurements in the rotor is advantageous. In addition, the experiences intended to detect incipient failure signs and threshold values for condition monitoring require a reconfigurable but still realistic machine, having an easy access and modifiable characteristics.

In this paper, the practical details related to the construction of the inverted motor as well as the results of the preliminary tests carried out on this machine are exposed.

## 1. Introduction

Exhaustive monitoring on the rotor of a squirrel cage induction motor is desirable as the models that simulate its behaviour become more detailed and require additional data to be validated. These data often demand a substantial precision and cannot be extrapolated. In addition, as new diagnosis methods have been developed, the necessity of confronting them with reality and to compare them with the standard ones arises. For those diagnostic procedures, as described in [1,2], it is especially important to know their capacity of following the evolution of defects from their very first steps and their ability to forecast adequately the behaviour of the equipment, and thus their expected remaining lifetime.
Although tests carried out on commercial motors can provide some answers, previous works [3] have established the complications that this approach faces due to the intrinsic difficulties in replicate an exact state of failure or reproduce a natural evolution of the fault.

The paper addresses both problems of evaluating new techniques of early fault recognition in induction motors, such as wavelet analysis, and providing data for detailed operational models by exhaustive measurements. For achieving these goals this paper proposes the design of a prototype of machine which allows an easy access to critical parts of it (as, for instance, the cage winding) and also an uncomplicated introduction of changes for simulating different kind of faults. The paper also describes the test bed used, the subsequent data storage system and the results of some tests which demonstrate the suitability of the prototype for the study of simulation and diagnostic approaches.

## 2. Design of the prototype of the inverted machine

Broken bar breakages are caused by a combination of thermal and mechanical loads in the rotor which damage preferment the joints between the bars and the rotor rings; therefore, to reproduce the process of degradation in the cage, the stator windings of a standard a 10 kW, 160L-size slip-ring induction motor has been substituted by a squirrel cage built by 36 trapezoidal aluminium bars; those bars have been shorted at both ends by an aluminium ring onto which they are screwed. The rotor windings, connected to the supply through the brushes and rings, act as primary winding, while the stator cage acts as secondary winding. This inverted disposition allows full access to the equivalent of the rotor cage winding in a commercial induction motor, which permits easier monitoring of the parameters of interest, including current and temperature [4].

TABLE I. – Motor characteristics

| | |
|---|---|
| V | 400 V –star (rotor) |
| P | 10 kW |
| I | 19.5 A |
| cos φ | 0.85 |
| rpm | 1460 |
| Th. Cl. | F |

Another advantage is constituted by the detachable configuration of the now static squirrel cage, which enables to perform modifications such as the insertion of damaged bars in order to artificially reproduce faults in various degrees, and the recording of data with the aim of assessing the viability of new techniques of analysis (Fig. 1). This disposition, in addition, avoids high mechanical stress on the reconfigurable cage, a drawback identified in previous works [5].

Fig. 1 – Bars placed in the stator slots.

A preceding study from the same group [4] has already established that the temperature in the stator core of an induction machine of this size equalizes rapidly for all points of the armature, with differences below 10 ºC in transient or 5ºC during stationary operation. Therefore, it was decided to place one thermocouple at the middle point of an already existing longitudinal hole along the stator in order to obtain a reference value.

That same study points out that the winding temperature differs further. In this case, there may exist an appreciable thermal resistance between the bars and the stator core since some clearance has to be left in order to allow its extraction (Fig. 2). For this reason, they will be monitored at both ends, with thermocouples attached using commercial thermal silicone rubber. The high aluminium conductivity ensures minor differences of temperature along the bars, thus discarding a significant gradient between the ends and the parts in contact with the armature. Similarly, other thermocouples will be installed on both short circuit rings.

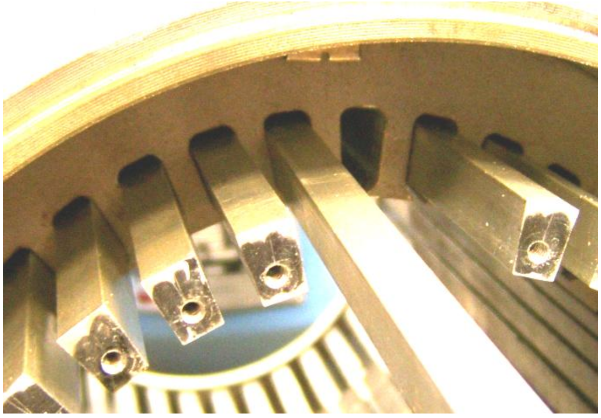

Fig. 2– Clearance between the stator armature and the bars

As Figure 3 shows, the cage has been built longer than the designed stator windings in order to have a better access to the rings and the ends of the bars, and to leave some clearance with the aim of installing current sensors around them.

Fig. 3– Stator of the inverted induction motor.

The section of the bars is 104.5 $mm^2$ (Fig. 4), and their length 360 mm. Both short circuit rings have an internal diameter of 160 mm, an external one of 225 mm and a width of 10 mm for a cross section of 650 $mm^2$. They are joint together by M4 aluminium screws which penetrate into the bars 9 mm. The resistance of each bar is estimated in $1 \cdot 10^{-7}\ \Omega$.

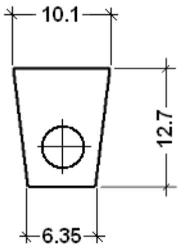


Fig. 4– Cross-section and dimensions (in mm) of a bar.

The longer bars and wide rings have prevented the use of the connection box for feeding the machine, thus, the brushes in the aft section are connected directly to the control and measurement devices (Fig. 5). Nevertheless, the connection box and associated empty spaces behind the stator core provide an easy path for instrumentation wires to reach the cage.

## 3. Description of the Test Bed, Control and Data Acquisition System

The inverted motor has been mounted on a wheeled lightweight frame having longitudinal slits and detachable joints for providing the flexibility needed for a rapid access to the cage. Further equipment is being studied to perform this operation *in situ*.

In order to carry out tests in its entire loading range, the motor is coupled to a 15 kVA alternator. Table II provides its main characteristics.

TABLE II. – Alternator characteristics

| | |
|---|---|
| V | 380 V –star |
| P | 15 kVA |
| I | 22.5 A |
| cos φ | 0.8 |
| rpm | 1500 |
| Th. Cl. | F |

The overall control of the induction motor and the alternator is performed by a PLC which allows for testing any working cycle of the induction machine. Data acquisition is achieved by a Yokogawa DL-750 multichannel recorder.

Fig. 5 – Test stand.

## 4. Results

The first tests were performed using a variable frequency drive. No problems were observed. Tables III and IV show the measurements taken from the standard no load and locked rotor tests.

TABLE III. No load test

| | |
|---|---|
| V | 386 V |
| I | 8.76 A |
| P | 702 W |
| Q | 5,793 VAr |
| PF | 0.11 |

TABLE IV. Locked rotor test

| | |
|---|---|
| V | 87 V |
| I | 19.29 A |
| P | 1,520 W |
| Q | 2,478 VAr |
| PF | 0.52 |

### *A. Motor internal parameters*

After performing unloaded and locked rotor tests, the following motor parameters have been calculated:

TABLE V. Measured internal parameters

| | |
|---|---|
| Rfe | 390 Ω |
| Xfe | 25.9 Ω |
| Zcc | 2.6 Ω |
| Rcc | 1.32 Ω |
| R'.st | 0.94 Ω |
| R.rot | 0.38 Ω |
| Xcc | 2.25 Ω |
| Xσ.st | 1.12 Ω |
| Xσ.rot | 1.12 Ω |
| Pmec | 232.1 W |
| Pfe | 381.7 W |

The results do not exhibit discrepancies from what it could be expected for an induction motor of that power.

### *B. Eccentricity detected*

The first current spectrum analyses of the machine performed under no load condition, clearly shows two components near 25 and 75 Hz (Fig. 6).

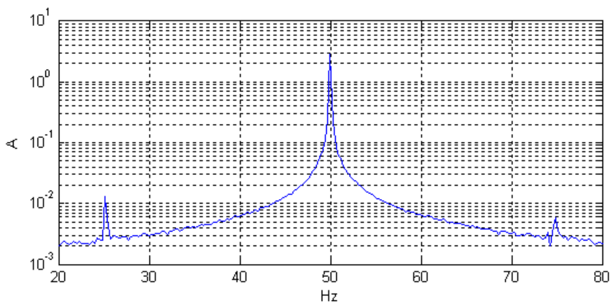


Fig. 6 – Stationary current spectrum.

According to [6], they correspond to the effect of a mixed eccentricity signature for a four pole, unloaded induction motor, as given by:

$$f_{ecc}^{*} = f_s \left(1 \pm k \cdot \frac{1-s}{p}\right) \qquad (1)$$

where $f^{*}_{ecc}$ is the characteristic frequency of the fault, $f_s$ is the supply frequency, $k$ is any positive integer, $s$ is the slip and $p$ the number of pole pairs. This defect might have been caused during the storage period of the rotor, in which it rested on both ends, while the cage was being designed, built and installed.

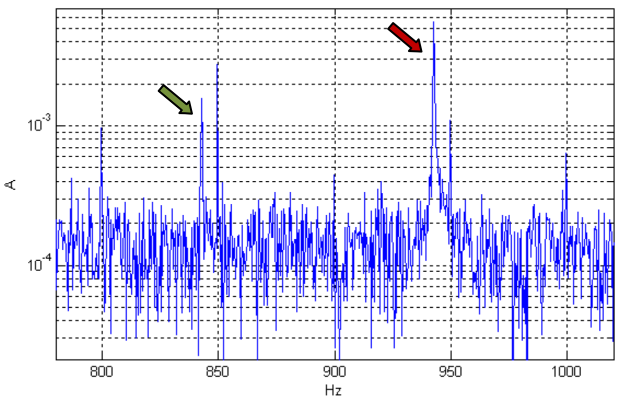


Fig. 7 –Principal slot harmonics +1 and -1

From the higher frequencies a similar diagnostic can be obtained. The right arrow in Figure 7 corresponds to the PSH+1 (Principal Slot Harmonic), whilst the left one is the PSH-1 for the unloaded machine, according to:

$$f_h = f_s\left((k \cdot R \pm n_d) \cdot \frac{1-s}{p} \pm \upsilon\right) \qquad (2)$$

where $f_s$ is the supply frequency, $k$ any positive integer, $R$ is the number of rotor slots, $n_d$ the eccentricity order, $s$ is the slip, $p$ the number of pole pairs and $\upsilon$ the order of the stator harmonics [7]. Since $n_d$ equals zero, it can be stated the presence of static eccentricity.

It is expected that it will not have effect in the study of rotor bar breakages.

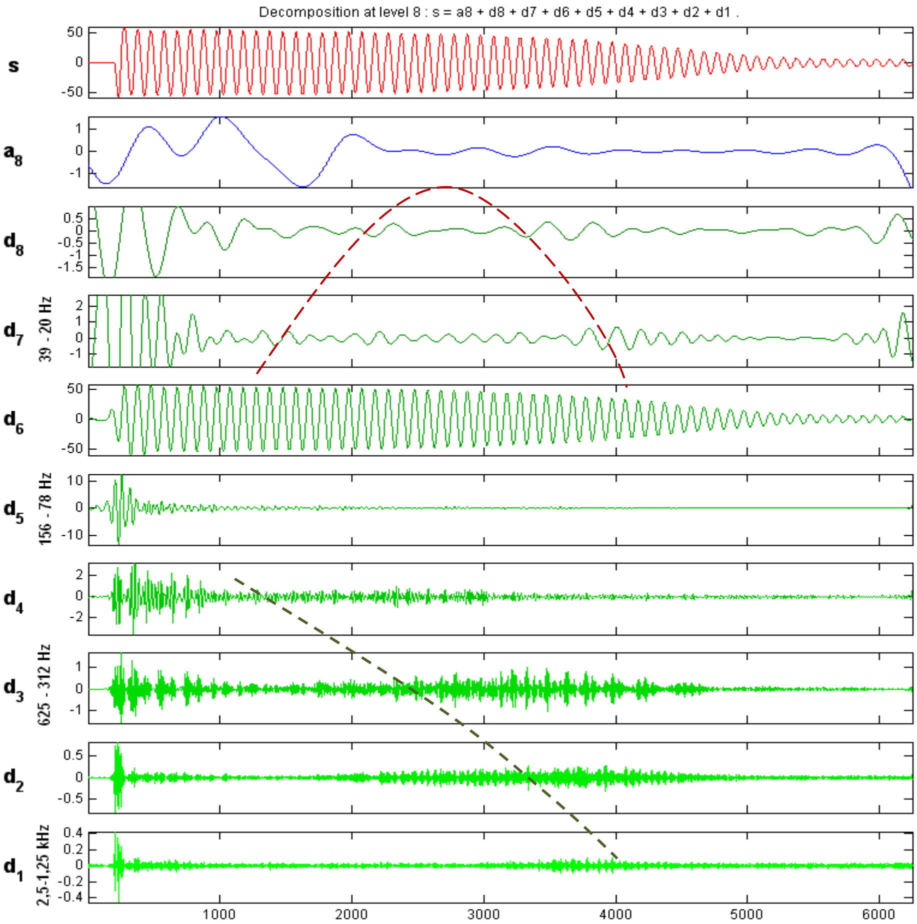


Fig. 8 –Wavelet decomposition of the current startup transient

*C. Asymmetry of the squirrel cage*

In order to evaluate the electrical symmetry of the constructed cage a start up test with reduced voltage has been carried out. The wavelet analysis of the primary current [8] is shown in Figure 8

It is appreciated in the seventh decomposition of the signal the harmonic related to the eccentricity, which evolves from 50 Hz to 25 Hz and therefore falls rapidly into this band. It is also detected superimposed in the seventh decomposition and in the eighth a slight stator cage asymmetry [8]. The evolution of the principal slot harmonics (PSH) is also observed in the decompositions that show frequencies above the main supply.

*D. Quantification of the asymmetry*

Since the characterization tests have been carried out at an unloaded condition, it is not possible to observe in the current spectrum the Left Sideband Harmonic (LSH) by means of applying directly the Fourier transform. Consequently, a new method of demodulation [9] using the Hilbert transform has been used. This method translates the main current component at the supply frequency to a DC one, which can be easily filtered, while the LSH appears now at a frequency equal to twice the slip, as shown in Figure 9:

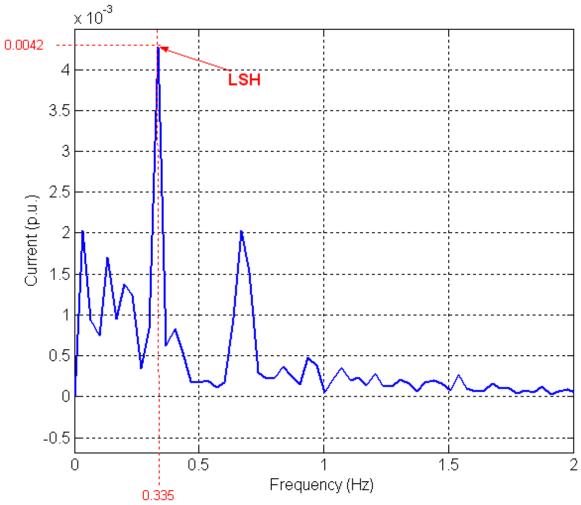


Fig. 9 –Improved current spectrum by the Hilbert method

From this result, the most widely used indicator, $\gamma_F$, which relates the amplitude of the fundamental harmonic ($I_1$) to that of the left sideband harmonic ($I_{Ls}$) is calculated:

$$\gamma_F(db) = 20 \cdot \log\left(\frac{I_1}{I_{Ls}}\right) \quad (3)$$

The value obtained, 47.5 dB, is well within the range of a healthy machine

A careful tightening of the aluminium screws joining the bars to the short circuit rings may minimize this effect.

## 5. Conclusions

This paper describes the constructive details and preliminary tests of a prototype of inverted induction cage motor set up in the Electrical Engineering Department of the Universidad Politécnica de Valencia.

Preliminary results indicate that the intended inverted induction machine suitable to be used to validate values of the rotor squirrel cage magnitudes and simulate rotor faults has been accomplished: The electrical parameters of the prototype resulting from the tests are similar to those of the commercial machines, and the easy access to the cage enables the direct measure of electrical, thermal and mechanical quantities.

Further work has to be carried out in order to furbish its stator cage with the sensors needed to monitor electric parameters before the research tests can begin.

## Acknowledgement


This work was supported by the Spanish “Ministerio de Educación y Ciencia”, in the framework of the “Programa Nacional de proyectos de Investigación Fundamental”, project reference DPI2008-06583/DPI


## References


[1] J.A. Antonino-Daviu, M.Riera-Guasp, J.Roger Folch,, M.P. Molina Palomares “Validation of a new method for the diagnosis of rotor bar failures via wavelet transform in industrial induction machines” *IEEE Trans. on Industry Applications*, vol. 42, no. 4pp .990-996, July/August 2006

[2] J.Antonino-Daviu, M.Riera-Guasp, J.Roger-Folch, F.Martínez-Jiménez, A.Peris,”Application and optimization of the discrete wavelet transform for the detection of broken rotor bars in induction machines” “*Applied and Computational Harmonic Analysis”* vol 21 no2 pp.268-279

[3] V. Climente-Alarcón, M.Riera-Guasp, J.Antonino-Daviu, J.Roger-Folch, “Experimental Study of the Evolution of a Bar Breakage Process in a Commercial Induction Machine” *Proceedings of the 2008 International Conference on Electrical Machines*

[4] G. Jiménez-Moreno, “Contribución al Estudio de las Máquinas Eléctricas Rotativas mediante el Método de los Elementos Finitos. Aplicación a la Máquina de Inducción” *PhD Thesis. Dept. Ingeniería Eléctrica, Universidad Politécnica de Valencia*, 1992

[5] Chia-Chou Yeh, Gennadi Y. Sizov, Ahmed Sayed-Ahmed, Nabeel A. O. Demerdash, Richard J. Povinelli, Edwin E. Yaz, Dan M. Ionel, “A Reconfigurable Motor for Experimental Emulation of Stator Winding Interturn and Broken Bar Faults in Polyphase Induction Machines” *IEEE Transactions on Energy Conversion*, Vol. 23, No. 4, December 2008

[6] S. M. A. Cruz, A. J. M. Cardoso and H. A. Toliyat, “Diagnosis of Stator, Rotor and Airgap Eccentricity Faults in Three-Phase Induction Motors Based on the Multiple Reference Frames Theory” *Conference Record of the Industry Applications Conference, 2003. 38th IAS Annual Meeting*. Vol. 2, pp. 1340-1346, 2003.

[7] S. Nandi, S. Ahmed, H. A. Toliyat, “Detection of Rotor Slot and Other Eccentricity Related Harmonics in a Three Phase Induction Motor with Different Rotor Cages”, *IEEE Transactions on Energy Conversion.* Vol. 16. No. 3, September 2001.

[8] J.A. Antonino-Daviu, M.Riera-Guasp, J.Roger Folch, M.P. Molina Palomares “Validation of a New Method for the Diagnosis of Rotor Bar Failures via Wavelet Transform in Industrial Induction Machines” *IEEE Trans. on industry applications*. Vol. 42, No. 4, pp. 990-996, July/August 2006

[9] R. Puche-Panadero, M. Pineda-Sanchez, *Member, IEEE*, M. Riera-Guasp, *Member, IEEE*, J. Roger-Folch, *Member, IEEE*, E. Hurtado-Perez, and J. Perez-Cruz. “Improved Resolution of the MCSA Method Via Hilbert Transform, Enabling the Diagnosis of Rotor Asymmetries at Very Low Slip” *IEEE Transactions on Energy Conversion.* Vol. 24. No. 1, March 2009.